JOURNAL OF MATERIALS SCIENCE 13 (1978) 239–242

Effects of moisture-assisted slow crack growth on ceramic strength

GIRRAJ K. BANSAL, WINSTON H. DUCKWORTH
Battelle, Columbus Laboratories, Columbus, Ohio 43201, USA

An investigation was made of strength degradation caused by moisture-assisted slow crack growth of surface flaws in two dense polycrystalline ceramics. Specimen sizes were varied. The observed strength degradation of each ceramic was predictable using K_{IC} as a material property in fracture-mechanics relations, suggesting that the only material variable involved was critical flaw size. The strength of one of the ceramics in water decreased significantly with increased specimen size, but its Weibull modulus was essentially unaffected by specimen size and slow crack growth.

1. Introduction

The strengths of many ceramic materials change with time in the presence of moisture because of slow crack growth. The velocity, V, of this growth in a water-bearing environment has been found related to stress-intensity factor, K_I, as follows [1]:

$$V = AK_I^n \quad (1)$$

where A and n are empirical material constants. If stressed at a constant rate, $\dot{\sigma}$, in the environment, slow crack growth is predicted to lower strength, σ_f, to the level given by the following relation [1]:

$$\sigma_f = \left[\frac{2\dot{\sigma}(n+1)}{A(Y/Z)^2(n-2)}\left(\frac{\sigma_{IC}}{K_{IC}}\right)^{(n-2)}\right]^{1/(n-1)} \quad (2)$$

where σ_{IC} is strength in the absence of slow crack growth, K_{IC} is the critical stress-intensity factor, and Y and Z are test-geometry and flaw-geometry parameters, respectively. During moisture-assisted slow crack growth from the surface, the flaw geometry tends to become semicircular [2]. For a semicircular surface flaw, $Z \simeq \pi/2$, and $Y \simeq 2$ [2].

In the investigation described below, effects of moisture-assisted slow crack growth on ceramic strengths were experimentally determined and compared with the prediction of Equation 2. For the prediction to hold, slow crack growth must enlarge the same flaws that initiate fracture in the absence of such growth. If different flaws are involved, strengths before and after the growth would be unrelated.

2. Experimental methods

Two dense commercial polycrystalline ceramics, a glass-ceramic*, and a sintered 95% Al_2O_3 ceramic†, were investigated. Strengths were determined in bend tests at room temperature using a special loading fixture and test procedures which minimized errors from spurious stresses [3]. Specimens were rectangular bars, all ground to an identical finish with a 320-grit diamond wheel. Two sizes of Al_2O_3 specimens were tested, 0.1 in. × 0.2 in. × 1.5 in. and 0.5 in. × 1.0 in. × 7.5 in. and the effective size of small specimens was further varied by using three- and four-point loading. Tests of the glass-ceramic were made using the smaller specimen and four-point loading.

Strength tests were conducted in dry N_2 at a stress rate of 100 MN m^{-2} sec^{-1} to restrict slow crack growth, and in distilled water at a stress rate of 4 MN m^{-2} sec^{-1} to enhance such growth.

Room temperature V–K_I data in distilled water and K_{IC} values were obtained by the double-torsion technique [4]. Rectangular bar specimens were grooved half the thickness to guide the crack and were precracked for these measurements.

*Pyroceram 9606, Corning Glass Works, Corning, New York (USA).
†Alsimag 614, Technical Ceramic Products Division, 3M Co., Chattanooga, Tennessee (USA).

TABLE I Strength test results

Material	Specimen size	Type of loading	Bend strength ($MN\,m^{-2}$)			
			Dry N_2		Water	
			Average*	Standard deviation	Average*	Standard deviation
Sintered Al_2O_3	Small	3-point	408 (8)	11.8	295 (15)	9.4
Sintered Al_2O_3	Small	4-point	369 (23)	16.6	271 (15)	9.5
Sintered Al_2O_3	Large	4-point	296 (10)	30.8	250 (5)	5.5
Glass-ceramic†	Small	4-point	317 (5)	7.0	204 (4)	3.1

*Number of specimens tested in parenthesis.
†Strength of this material showed no dependence on specimen size or type of loading when fracture originated at the surface [5]; thus, the strength values given are considered generally applicable.

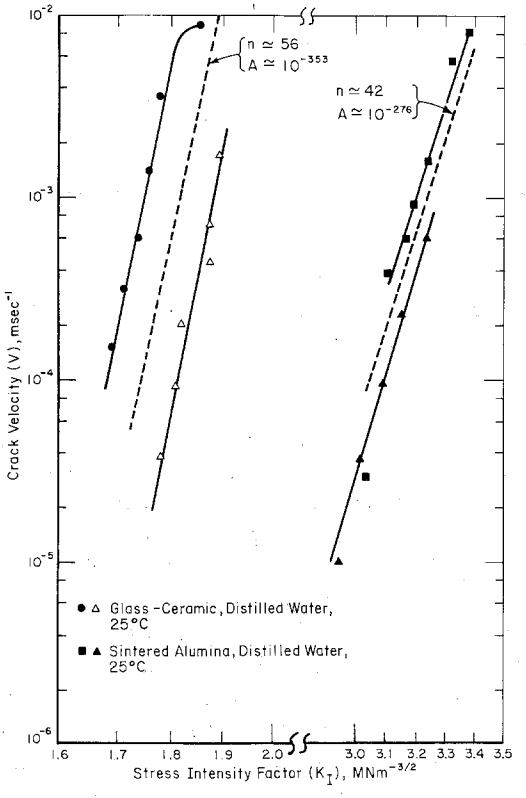

Figure 1 Crack velocity as a function of stress intensity factor.

3. Experimental results

Fractographic examinations revealed that fracture in specimens of both materials initiated at surface sites when tested in water. Some specimens tested in dry N_2, however, exhibited subsurface fracture origins, the frequency of these origins increasing with specimen size [5, 6]. Because slow crack growth associated with ambient moisture would occur from the surface, strength data from specimens with subsurface fracture origins are irrelevant to the question of effects of such growth on strength. Accordingly, sets of strength data from tests in dry N_2 containing values from subsurface flaw failures have not been considered here, but were considered in interpreting strength–size relations exhibited by the specimens, reported elsewhere [5, 6].

Table I summarizes the strength data for both materials. K_{IC} values obtained on four specimens each of the glass-ceramic and sintered Al_2O_3 were 2.38 ± 0.08 and 3.84 ± 0.05, respectively. V–K_I plots obtained from two specimens of each material are given in Fig. 1. The plots show that the expected relation, Equation 1, describes the observed crack growth rates in water reasonably well with A and n having average values of 10^{-353} and 56 respectively, for the glass-ceramic, and 10^{-276} and 42 for the sintered Al_2O_3. The differences in the two sets of experimental data for each material are largely associated with experimental errors in determining crack velocities, since, as noted above, little scatter was measured in K_{IC} values.

4. Discussion

Table II compares predicted and observed strengths in water. Average strengths in dry N_2 were used for σ_{IC} in Equation 2 to obtain the predicted strengths, σ_f, except for the large Al_2O_3 specimens. In this case, because fracture in dry N_2 invariably originated at subsurface sites, no experimentally-determined strength was available for σ_{IC}, so Weibull statistics [7] were empolyed to obtain the σ_{IC} value as follows:

Weibull plots of the strength data from Al_2O_3 specimens fracturing from surface origins are presented in Fig. 2. These plots are for probabilities of failure ranging at most from about 0.05 to 0.95.

TABLE II Calculated and measured strengths in water

Material	Specimen size	Type of loading	Average strength ($MN\,m^{-2}$)	
			Measured	Predicted
Sintered Al_2O_3	Small	3-point	295	288
Sintered Al_2O_3	Small	4-point	271	263
Sintered Al_2O_3	Large	4-point	250	243*
Glass-ceramic	Small	4-point	204	210

*Calculated on the basis of strength in dry N_2 obtained from Weibull statistical relations (see text).

Each plot is reasonably linear, indicating that the Weibull two-parameter form describes the data; (i.e. the stress for which there is zero probability of failure can be taken to be zero).

As noted in Fig. 2, the plots give Weibull moduli, m, of 34 for each testing condition except when small specimens were tested with four-point loading in dry N_2, in which case the m value was not greatly different, being 26. These results suggest that for each test condition flaws from the same statistical population were responsible for failure.

Weibull statistics [7] gives the following relation between average strength and specimen size when the failure results from surface flaws:

$$\bar{\sigma}_1/\bar{\sigma}_2 = (S_2/S_1)^{1/m} \quad (3)$$

where S is the effective surface area and subscripts 1 and 2 refer to different specimen sizes. From Equation 3, with $m = 34$, $\bar{\sigma}_1/\bar{\sigma}_2 = 1.10$ for the strength ratio between the small and large specimens when both are tested with four-point loading ($S_2/S_1 = 25$). The ratio agrees favourably with the experimentally observed ratio of 10.8 from tests in water (Table I), and suggests that the large specimens tested in dry N_2 would have exhibited an average strength of $369/1.10 = 335\,MN\,m^{-2}$ if surface flaws had controlled their failure*. Accordingly, a value of $335\,MN\,m^{-2}$ was used for σ_{IC} in Equation 2 to obtain the predicted strength given in Table II for large specimens in water.

5. Conclusions

The applicability of Equation 2 for predicting strengths in water, shown by the excellent agreement with measured strengths in Table II, indicates that the following conditions prevailed:

(1) Little or no slow crack growth occurred during the strength tests in dry N_2.

(2) Slow crack growth during strength tests in water initiated from the same flaws that were responsible for fracture in dry N_2 in the absence of subsurface origins.

(3) K_{IC} of each material behaved as a bulk property, independent of the ambient and/or microstructural features at the local site where

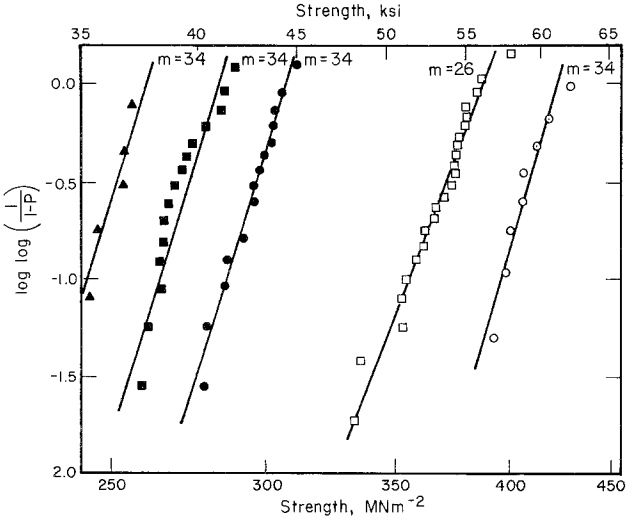

Figure 2 Weibull plots of strength–size data for sintered Al_2O_3.

Environment		
Water	Dry N_2	
▲		4-point large
■	□	4-point small
●	○	3-point small

*Subsurface flaws caused the measured average strength in dry N_2 to be $296 \pm 31\,MN\,m^{-2}$ [6].

fracture or slow crack growth originated. Subsequent investigations of other aluminas [8, 9], however indicate that K_{IC} could also vary depending on environmental conditions, and variations in both the critical flaw size and K_{IC} should be considered in predicting strengths using fracture mechanics. (K_{IC} was determined from the strain energy release rate when a large artificial crack became unstable.)

The equivalence of Weibull moduli from tests of Al_2O_3 in dry N_2 and water adds support to the above indication that flaws from the same population controlled fracture in the presence and absence of slow crack growth, and no variable other than critical flaw size influenced strength degradation in water. In considering applicability of Weibull statistics, it is important to point out that the strength data gave failure probabilities in a limited range, 0.05 to 0.95. Had the probability ranges been extended sufficiently by tests of additional specimens, subsurface flaw failures no doubt would have altered the strength–probability relationship, perhaps sufficiently to make the Weibull statistical approach unsuited for calculating the σ_{IC} value unless specimens exhibiting subsurface flaw failures were identified and data from them excluded from the analysis.

Acknowledgement

The research was sponsored by the Office of Naval Research under Contract No. N00014-73-C-0408, NR 032-541, monitored by Dr A. M. Diness.

References

1. A. G. EVANS and H. JOHNSON, *J. Mater. Sci.* **10** (1975) 214.
2. G. K. BANSAL, *J. Amer. Ceram. Soc.* **59** (1976) 87.
3. R. G. HOAGLAND, C. W. MARSCHALL and W. H. DUCKWORTH, *ibid* **59** (1976) 189.
4. D. P. WILLIAMS and A. G. EVANS, *J. Test. Eval.* **1** (1973) 264.
5. G. K. BANSAL, W. H. DUCKWORTH and D. E. NIESZ, *Bull. Amer. Ceram. Soc.* **55** (1976) 189.
6. G. K. BANSAL, W. H. DUCKWORTH and D. E. NIESZ, *J. Amer. Ceram. Soc.* **59** (1976) 472.
7. D. G. S. DAVIES, *Proc. Br. Ceram. Soc.* **22** (1973) 429.
8. H. HÜBNER and W. JILLEK, *J. Mater. Sci.* **12** (1977) 117.
9. G. K. BANSAL and W. H. DUCKWORTH, *J. Mater. Sci.* **13** (1978) 215.

Received 7 January and accepted 2 May 1977.